Research Article

Journal of PeptideScience

Received: 14 May 2011 Revised: 10 September 2011 Accepted: 13 September 2011 Published online in Wiley Online Library

(wileyonlinelibrary.com) DOI 10.1002/psc.1424

Effect of introducing a short amyloidogenic sequence from the Aβ peptide at the N-terminus of 18-residue amphipathic helical peptides

Chandrasekaran SivakamaSundari, Sridharan Rukmani and Ramakrishnan Nagaraj*

Fibril formation is the hallmark of pathogenesis in Alzheimer's disease and other amyloid disorders caused by conformational alterations leading to the aggregation of soluble monomers. Aβ40 self-associates to form amyloid fibrils. Its central seven-residue segment KLVFFAE (Aβ16–22), which is thought to be crucial for fibril formation of the full-length peptide, forms fibrils even in isolation. Context-dependent induction of amyloid formation by such sequences in peptides, which otherwise do not have that propensity, is of considerable interest. We have examined the effect of introducing the Aβ16–22 sequence at the N-terminus of two amphipathic helical 18-residue peptides Ac-WYSEMKRNVQRLERAIEE-am and Ac-KQLIRFLKRLDRNLWGLA-am, which have high average hydrophobic moment $<\mu H>$ values but have net charges of 0 and +4, respectively, at neutral pH. Upon incubation in aqueous buffer, fibril-like aggregates were discernible by transmission electron microscopy for the peptide with only 0 net charge, which also displayed ThT binding and β-structure. Although both the sequences have been derived from amphipathic helical segments in globular proteins and possess high average hydrophobic moments, the +4 charge peptide lacks the ability to form fibrils, while the peptide with 0 charge has the tendency to form fibrillar structures. Variation in the net charge and the presence of several glutamic acids in the sequence of the peptide with net charge 0 appear to favor the formation of fibrils when the Aβ16–22 sequence is attached at the N-terminus. Copyright © 2011 European Peptide Society and John Wiley & Sons, Ltd.

Keywords: Alzheimer's disease; amphipathic helices; fibrillar structure; peptide nanostructures; self-association

Introduction

Hydrophobic interactions are one of the major driving forces that play a key role in many processes in biology, particularly in the formation of self-assembled structures. Peptides that form amphipathic helices in solvents such as TFE, micelles and lipid vesicles self-associate to form oligomeric structures composed of helical bundles, particularly in membrane environment. Examples include melittin [1], delta-lysin [2,3] and pardaxin [4,5]. Alamethicin, although not amphipathic, also forms oligomeric aggregates [6–8]. However, helical amphipathic peptides do not form amyloid fibrils. If a helical peptide can be induced to form cross-beta structures, then amyloid fibrils are observed [9–11]. In proteins that form amyloid fibrils, small segments in them have the ability to form amyloid fibrils in isolation that are indistinguishable from fibrils formed by the parent protein [12–24]. The context dependence of amyloid induction by amyloidogenic sequences, that is, whether short amyloid-forming peptides can induce fibril formation when attached to peptides that do not have the propensities to fold into β-structures, is yet to be established unequivocally.

Self-assembly of peptides that are segments of amyloidogenic proteins and their variants has been the subject of extensive investigations with a view to delineate the physicochemical properties that govern self-assembly. The peptide KLVFFAE (Aβ16–22) spanning the central 16–22 region of Aβ40 has been shown to form either fibrils or nanotubes, depending on pH [12,13,25–28]. This peptide forms oligomeric antiparallel β-sheets at neutral pH, where there would be charge complementarity of the N and C termini [13]. The self-assembly of peptides generated from the segment KFFE indicates that their amyloidogenic properties are strongly dependent on the structural environment of the peptide, with random or β-hairpin conformations not favoring fibril formation [29]. Molecular dynamics simulations of the shorter variants of Aβ40 also indicate that short segments from the entire sequence play an important role in the formation of β-sheets and thereby modulate aggregation [30]. Although there are several studies describing the disruption or inhibition of amyloid formation by using shorter peptides or hydrophobic peptide analogs derived from this same oligomer Aβ16–22, there are no reports available wherein other peptide structural motifs have been employed to influence fibrillogenesis. Short cationic peptides with homologous recognition sequences have been shown to inhibit the aggregation that occurs because of the structural transition [31]. Two inhibitor peptides, iAβ5 and iAβ5^{inv}, with primary structures LPFFD and DPFFL respectively, containing the β-sheet-beaker

* *Correspondence to: Ramakrishnan Nagaraj, Centre for Cellular and Molecular Biology, Uppal Road, Hyderabad 500 007, India. E-mail: nraj@ccmb.res.in*

CSIR-Centre for Cellular and Molecular Biology, Uppal Road, Hyderabad 500 007, India

Abbreviations used: *ANS, 1-anilinonaphthalene-8-sulfonic acid; CD, circular dichroism; HEPES, 2-[4-(2-hydroxyethyl)-1-piperazine]-ethanesulfonic acid; HPLC, high-performance liquid chromatography; MeOH, methanol; MRE, mean residue ellipticity; PDB, Protein Data Bank; SDS, sodium dodecyl sulfate; ThT, Thioflavin T; TEM, transmission electron microscopy; TFA, trifluoroacetic acid; TFE, 2,2,2-trifluoroethanol.*

Journal of PeptideScience

proline, have been used wherein their structural models bound to fibrillar Aβ14–23 and Aβ1–40 suggest interactions involving the hydrophobic core residues K16 and E22/D23 of the Aβ sequence [32]. Therefore, it would be of interest to examine whether short peptides from the Aβ sequence can form amyloid fibrils in the presence of structural motifs such as amphipathic helices. We had earlier analyzed the PDB for the occurrence of 18-residue amphipathic helical segments from globular proteins [33,34]. In this study, we have investigated the aggregation behavior of two 18-residue amphipathic helical peptides with high average hydrophobic moments, having cationic and anionic amino acids with net charges of 0 and +4 at neutral pH, when the Aβ16–22 sequence is introduced at their N-terminus. The sequences of the peptides are as follows: Pc3c, Ac-WYSEMKRNVQRLERAIEE-am (0), Pill, Ac-KQLIRFLKRLDRNLWGLA-am (+4), Nab-Pc3c, Ac-KLVFFAE WYSEMKRNVQRLERAIEE-am (0), Nab-Pill, Ac-KLVFFAEKQLIRFLKRLD RNLWGLA-am (+4). The net charge at neutral pH is indicated in parentheses.

Materials and Methods

Materials

Fmoc amino acids were purchased from Advanced ChemTech (Louisville, KY, USA) and Novabiochem AG (Laufelfingen, Switzerland). Peptide synthesis macrocrowns were purchased from Mimotopes, Australia. All other reagents were of highest grade available. ThT and ANS were obtained from Sigma (St. Louis, MO, USA).

Peptide Synthesis

Peptides were synthesized on C-terminal amide-containing macrocrowns manually by employing Fmoc chemistry [35]. They were cleaved from the crowns using TFA containing water, phenol, thioanisole and ethanedithiol (82.5:5.0:5.0:5.0:2.5 v/v) for 12–15 h at room temperature (RT) [36]. Peptides were purified by HPLC using a Hewlett-Packard 1100 series HPLC (Hewlett-Packard, Waldbronn, Germany) instrument on a reverse phase C-18 column (Bio-Rad, Richmond, CA, USA) using gradients of (i) 0.1% TFA in water and (ii) 0.1% TFA in acetonitrile. Further characterization was carried out by matrix-assisted laser desorption/ionization time-of-flight mass spectrometry on Voyager DE STR mass spectrometer (PerSeptive Biosystems, Foster city, CA, USA) by using α-cyano-4-hydroxycinnamic acid as the matrix. The *m/z* values (calculated values in parentheses) observed were as follows: Nab-Pc3c, 3214.9 (3214.6 Da), Nab-Pill, 3119.1 (3118.7 Da), Pc3c, 2379.1 (2379.6 Da), and an *m/z* value of 2284.3 (2283.7 Da) was obtained for Pill.

Peptide Solutions

Concentration of the peptide stocks in MeOH were as follows: Pc3c, 2.4 mM; Pill, 430 μM; Nab-Pc3c, 930 μM and Nab-Pill, 320 μM. These stock solutions were stored at 4 °C. TEM images from MeOH solutions did not indicate organized structures. Therefore, the MeOH was evaporated and the peptides were redissolved in TFE for TEM. For incubation in aqueous buffer (5 mM HEPES, pH 7.4), samples were prepared from MeOH stocks by concentrating to a fixed small volume of MeOH, followed by dilution with aqueous buffer prior to incubation. The total content of MeOH was less than 5% in all cases. Appropriate controls of buffer/MeOH were also included in all the experiments. Correction of the spectra was performed by subtraction of this control from the sample wherever necessary. Similarly, grids treated with this incubated control solution have been viewed by TEM and found to be blank.

Transmission Electron Microscopy

Samples were prepared by dipping/layering the peptide solution aliquoted from the stocks on the copper grid coated with carbon. After drying the solvent by blotting, the grids were dipped into a drop of uranyl acetate, and the excess solution was removed by blotting. These grids were viewed under the electron microscope up to a maximum magnification of 20 000. The images were obtained using a JEM-2100 transmission electron microscope (JEOL, Tokyo, Japan) at 100 kV.

ThT Binding to Monitor Fibril Formation

Thioflavin T fluorescence assay was performed using a modification of the method described by Naiki *et al.* [37]. Aliquots from 200 μM peptide solutions incubated for 27 days in buffer with and without 150 mM NaCl were added to ThT (10 μM) in 50 mM phosphate buffer, pH 7.4 to yield a final peptide concentration of 20 μM. Fluorescence spectra were recorded on a Fluorolog-3 Model FL3-22 spectrofluorometer (Horiba Jobin Yvon, Park Avenue Edison, NJ, USA) between 460 and 550 nm. The excitation wavelength was set at 450 nm, excitation slit width at 2 nm and emission slit width at 5 nm.

ANS Fluorescence

In order to monitor the generation of any possible hydrophobic surfaces due to the aggregation of the peptides in buffer upon increase in concentration, they were titrated into 5 μM ANS. Increasing amounts of the peptide stocks were added to a solution of 5 μM ANS in 5 mM HEPES buffer, pH 7.4. Emission spectra were recorded between 400 and 600 nm with band widths of 5 nm and excitation wavelength set at 365 nm. Blank spectra of solutions containing corresponding amounts of the peptides were subtracted. All measurements were carried out on a Hitachi 4500 fluorescence spectrometer (Hitachi, Tokyo, Japan). The wavelength of maximum emission and the intensity of fluorescence were plotted as a function of peptide concentration.

CD Measurements

Spectra were recorded in 5 mM HEPES buffer, pH 7.4 with and without SDS on a JASCO-J-815 spectropolarimeter (Jasco, Tokyo, Japan) using a quartz cell of 1 mm path length at 25 °C. The spectra were recorded by averaging eight scans and corrected by subtracting the blank buffer or SDS spectra. MRE was calculated using the formula $[\theta]_{MRE} = (M_r \times \theta_{mdeg})/(100 \times l \times c)$,where M_r is mean residue weight, θ_{mdeg} is ellipticity in millidegrees, l is path length in decimeter and c is the peptide concentration in mg ml^{-1}. Data are represented as MREs. Peptide concentration = 50 μM. SDS concentration = 20 mM.

Results

The retention times (min) of the peptides on a C-18 reversed phase column during HPLC analysis were Pc3c: 24.71, Pill: 26.95, Nab-Pc3c: 26.3 and Nab-Pill: 32.02, respectively. The values

indicate increase in hydrophobicity of the 25-residue peptides. Peptide Pc3c, although it has a net charge of 0 at neutral pH, is composed of four cationic amino acids and four anionic amino acids. Pill has five cationic amino acids and one anionic amino acid.

Transmission Electron Microscopy

Transmission electron microscopy images of peptides (200 μM) redissolved in TFE are shown in Figure 1. Pc3c displayed circular structures with diameter ranging from 10 to 50 nm, as well as equal number of smaller spherical balls with diameter around 5 nm that were clustered. Pill formed larger spherical structures having diameter varying from 10 nm to a maximum of around 85 nm. The larger balls were found to be around 20% of the total population. Nab-Pc3c formed short, elliptical lumps of 10 nm thickness adhering to each other and growing in all the directions. Bunches were discernible wherever the density was high. Nab-Pill formed a mesh-like pattern, with grids of 10 nm thickness.

Transmission electron microscopy images of Nab-Pc3c were recorded at different time points during the incubation in 5 mM HEPES buffer, pH 7.4, at RT (Figure 2A–D). Self-assembly of Nab-Pc3c (200 μM), the peptide with net charge of 0, appears to get triggered even at early time points. Ordered structures are perceptible by 19 h, which entangled to form bundles (Figure 2A) and progressed to dense networks with time when incubated up to 98 days (Figure 2B–D). Inclusion of 150 mM NaCl during the incubation of Nab-Pc3c also resulted in similar fibril-like structures as shown in Figure 2(E). Concentration-dependent dense networks were also seen. At a higher concentration of 400 μM (Figure 2F), the fibril bundle appears to be more dense, with diameter values in the range similar to the 200 μM sample (Figure 2C) of 4–10 nm. Images of Pc3c, Pill and Nab-Pill redissolved in 5 mM HEPES buffer to a final concentration of 200 μM and kept for 10 days at RT are shown in Figure 3. Pc3c shows dense mesh-like assembly. Pill and Nab-Pill show nodular oval-shaped short structures, which are joined. The structures are different from those observed for Nab-Pc3c.

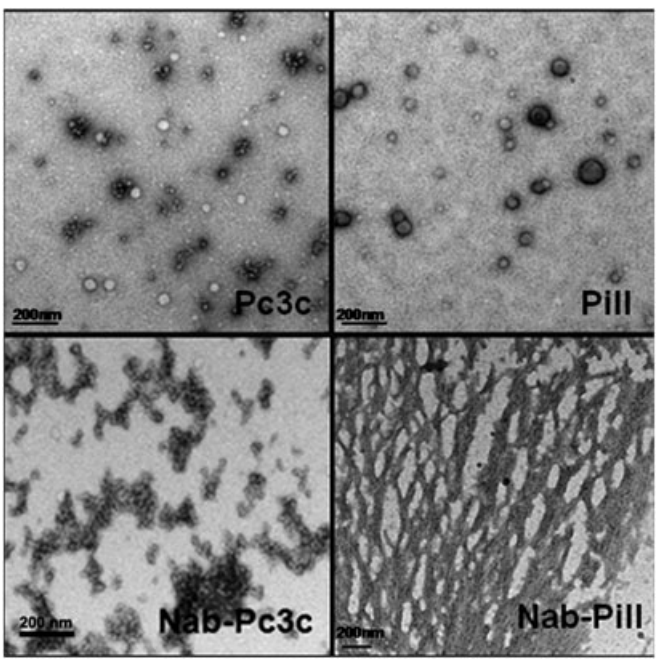

Figure 1. TEM images of dry peptide films obtained from TFE. Peptides were dried from their original stock solutions and redissolved in TFE to an identical concentration of 200 μM and layered on copper grids for TEM studies.

The ThT fluorescence of peptide solutions left for incubation at RT in 5 mM buffer was checked after further incubation. For the 27 days-incubated sample, it was found that the parent 18-mer peptides and Nab-Pill do not show any increase in ThT fluorescence suggesting absence of amyloid fibrillar structures (data not shown). Enhancement of ThT fluorescence at 510 nm is discernible in Nab-Pc3c (Figure 4). Emission peak between 510 and 520 nm has been observed for fibrils formed by Aβ1–42 [38,39], human amylin [40] and a short 5-residue peptide [41].

ANS Fluorescence

1-Anilinonaphthalene-8-sulfonic acid has been used to monitor hydrophobic regions in self-assembled structures [42,43]. Changes in the fluorescence properties of ANS upon titration with peptides in buffer are shown in Figure 5 as a function of the peptide concentration. Pc3c, although amphipathic, does not seem to facilitate ANS binding. In contrast, the other peptides appear to form hydrophobic pockets/sites for ANS binding, from the observed changes both in the emission maximum as well as the F/F_0 ratio. As shown in Figure 5A, the emission maximum of ANS, which is around 515–520 nm in aqueous buffer, undergoes a considerable blueshift (up to 50 nm) to 467 nm in the presence of the three peptides. There is a concomitant pronounced enhancement in the fluorescence intensity (Figure 5B) indicative of a strong binding. While the fold increase is around 5 in Pill, a further increase is observed in Nab-Pill almost up to an F/F_0 value of 12. Attaching Aβ16–22 appears to increase the available hydrophobic surfaces facilitating ANS binding in the case of the 25-mers as compared with the parent 18-mer peptides. Despite the similar behavior exhibited by Pill, Nab-Pill and Nab-Pc3c to bind ANS in buffer from freshly prepared solutions, Nab-Pc3c appears to self-associate into fibrillar assemblies in less than 24 h.

Secondary Structure

Far UV CD spectra of the peptides in 5 mM HEPES buffer and SDS micelles are shown in Figure 6(A–D). In buffer, the spectra suggest that the peptides are largely unordered. The presence of Aβ16–22 at the N-terminus does not prevent the peptides Nab-Pill and Nab-Pc3c from adopting α-helical conformation in a membrane-mimetic environment, such as micelles of SDS. The structures of Pc3c, Pill as well as the longer peptides show α-helical conformation in SDS micelles. Addition of Aβ16–22 at the N-terminus does not 'force' the peptides into β-conformation. We had earlier shown that Pill and Pc3c adopt helical conformation in the structure-inducing solvent TFE [33]. Far UV CD spectrum from an aliquot of Nab-Pc3c sample diluted to 30 μM (incubated for 40 days when CD was recorded) exhibits a negative band with a minimum centered at around 216–218 nm (inset in Figure 6C), characteristic of beta-sheet conformation.

Discussion

Hydrophobic interactions have been implicated to play an important role during oligomerization in amyloidogenesis [12,26,44–46]. Several studies on self-aggregating peptides and proteins have demonstrated the presence of at least a few hydrophobic residues, particularly aromatic residues, in the region that is

Journal of PeptideScience

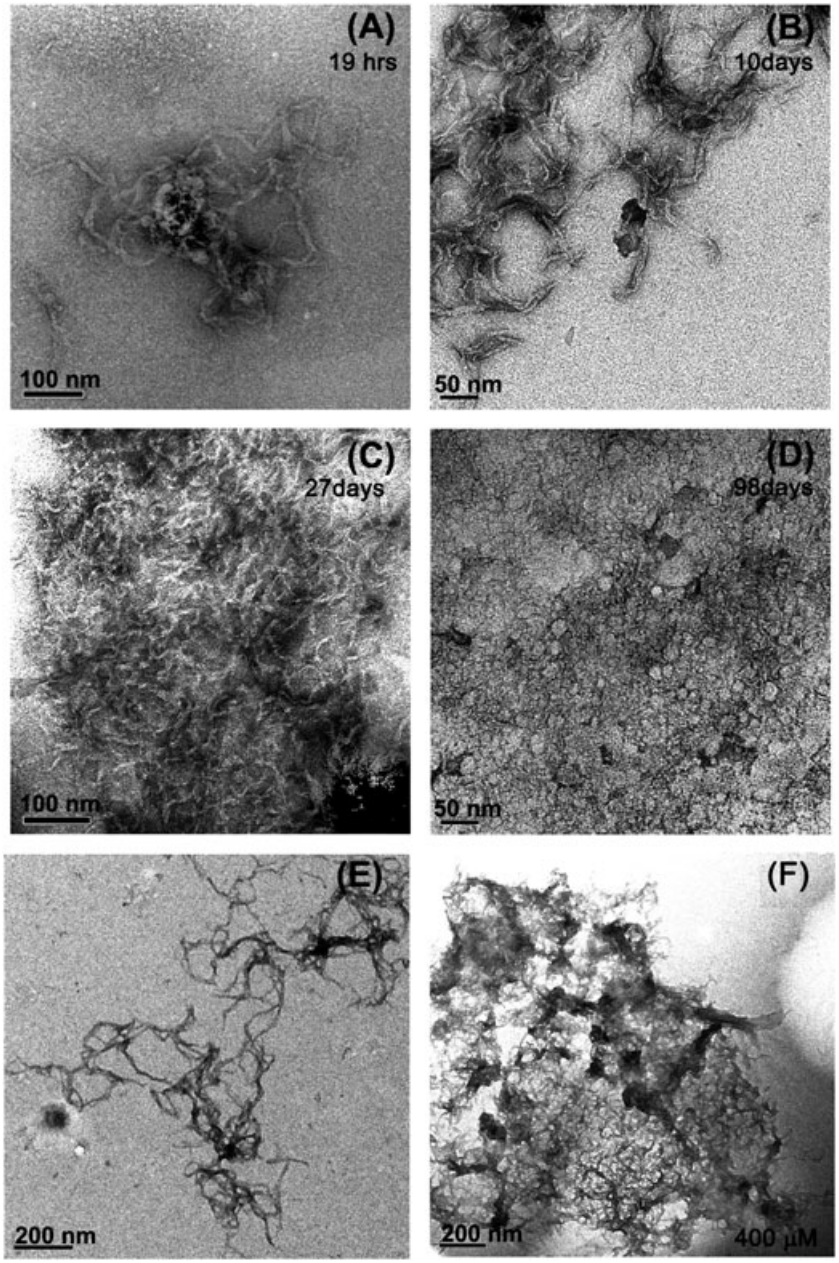

Figure 2. TEM images of Nab-Pc3c in buffer. (A–D) Structure formation in 200 μM peptide as a function of incubation time, (E) after incubation in 150 mM NaCl for 10 days at RT and (F) structure formation in 400 μM peptide after incubation in buffer for 27 days at RT.

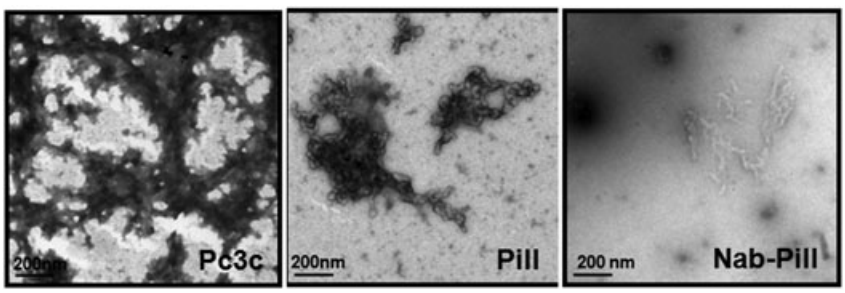

Figure 3. TEM images of 200 μM of Pc3c, Pill and Nab-Pill in buffer after incubation for 10 days at RT.

susceptible to form amyloids [44–48]. Our interest was to see whether the two 18-mer amphipathic helical segments when attached to the C-terminus of Aβ16–22 can exert their effect on fibrillation, as they possess high hydrophobic moment values. Analysis on reversed phase HPLC shows that Nab-Pill elutes at a higher % of acetonitrile–water at 66% when compared with

Nab-Pc3c (54.7%), indicating greater hydrophobicity for Nab-Pill as compared with Nab-Pc3c. We investigated whether this increased hydrophobicity would eclipse the electrostatic interactions that may be different because of the difference in net charge. The different morphologies of the aggregates between the 18-mer and 25-mer peptides indicate that the self-association during the drying process is different, which could arise because of the increased hydrophobicity of Nab-Pc3c and Nab-Pill. ANS binding data (Figure 5) provide further evidence that both the 25-mer peptides form aggregates that facilitate ANS binding. The higher F/F_0 values as compared with their respective 18-mer parent peptides suggest increase in hydrophobicity. Studies on hydrophobically modified amyloid peptide fragments of KLVFF have shown fibrillization of FFKLVFF in MeOH [49], whereas AAKLVFF forms nanotubes [50]. Fibril formation of a 13-residue peptide Ac-DWSFYLLYYTEFT-am (Pβ2m) was observed to depend on the organic solvent in which peptide stock solutions were prepared, whereas in buffer, β-structure was observed irrespective of the solvent in which the peptide stock solutions were prepared [51]. Influence of the solvent has been demonstrated to cause structural differences on the self-assembly of AAKLVFF, the modified peptide fragment of the central Aβ16–22 KLVFF [52,53]. In another study, although the two peptides KhK (KKKFLIVIGSIIKKK) and alternating Kh (KFLKKIVKIGKKSII) possess similar overall hydrophobicity, isoelectric points and amino acid content, local differences in the ability to form hydrophobic and electrostatic interactions within and among peptide chains caused inverse behavior of peptide solutions on HDPE substrates [54]. Three different types of ionic peptides EAK16-I, EAK16-II and EAK16-IV, which have the same amino acid composition but different amino acid sequences, were studied, where atomic force microscopy confirms that two types EAK16-I and EAK16-II form fibrillar assemblies, whereas the third type EAK16-IV forms globular structures [55].

In the present study, the different morphologies of the aggregates between the 18-mer and 25-mer peptides indicate that with the exception of Pc3c, the peptides aggregate in aqueous medium. However, the self-association during the drying process

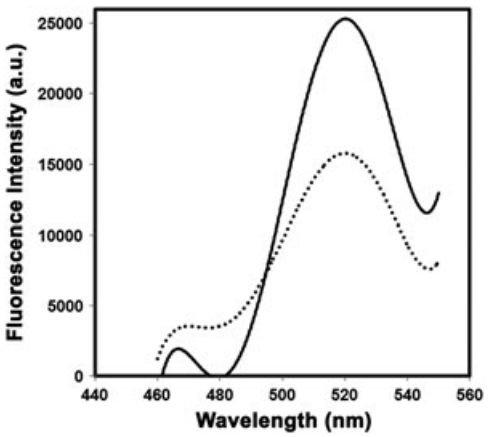

Figure 4. ThT fluorescence spectra of Nab-Pc3c incubated for 27 days in 5 mM HEPES buffer (solid) and in buffer + 150 mM NaCl (dotted). Fluorescence spectra were recorded between 460 and 550 nm with the excitation wavelength set at 450 nm. ThT concentration = 10 μM. Final peptide concentration was 20 μM in 50 mM phosphate buffer, pH 7.4.

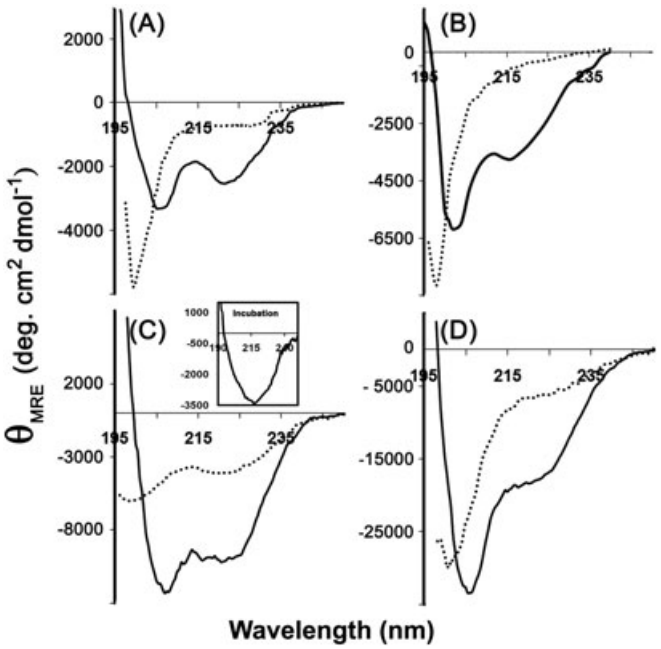

Figure 6. Far UV CD spectra of peptides prepared freshly in buffer (dotted) and SDS micelles (solid): (A) Pc3c, (B) Pill, (C) Nab-Pc3c and (D) Nab-Pill. Inset in panel C shows the spectrum of Nab-Pc3c, after incubation for 40 days in buffer, at RT. From the incubated sample of Nab-Pc3c (200 μM), an eightfold dilution was performed to achieve 25 μM for recording the CD spectrum.

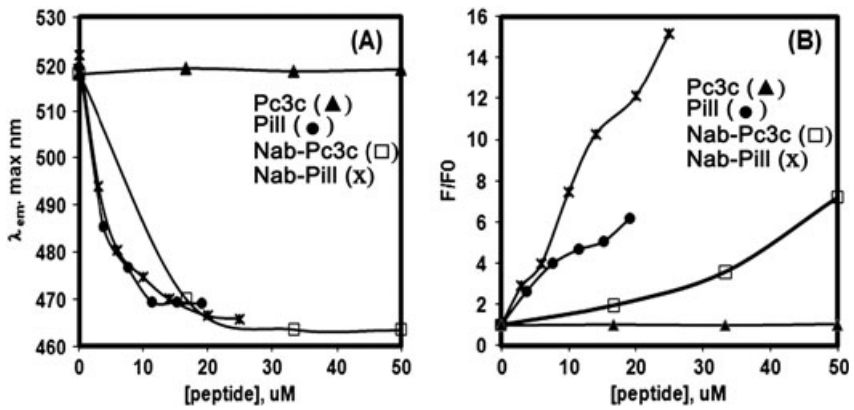

Figure 5. ANS binding to peptides in buffer. Panel (A) represents the blueshift in $\lambda_{em.}$ maximum as a function of peptide concentration. Panel (B) represents the changes in the fluorescence intensity with increase in peptide concentration. ANS = 5 μM. $\lambda_{ex.}$ = 365 nm.

Journal of PeptideScience

is different, which could arise because of the increased hydrophobicity of Nab-Pc3c and Nab-Pill. Charge attraction and propensity to form β-structures have been shown to be essential for fibril formation [29]. Nab-Pill and Nab-Pc3c vary in their net charges at neutral pH. Nanostructure formation was observed only in Nab-Pc3c after incubation for 10 days. Upon close examination of the two peptide sequences, it is observed that the distribution of cationic residues along the sequence is similar in both the peptides; the dissimilarity is the lack of glutamic acids in Pill, while Pc3c has four glutamic acids, one closer to the N-terminal portion beside a dense cluster of three residues at the C-terminus. Fibril formation in Nab-Pc3c appears to be facilitated irrespective of the presence or absence of 150 mM NaCl. Castelletto *et al*. have studied the effects of NaCl on the self-assembly of AAKLVFF and βAβAKLVFF in solution and have attributed the differences in morphology to the progressive screening of the surface charge caused by the addition of salt [56]. In another study, a designed simple amphiphilic peptide V6D sequence has six hydrophobic valine residues from the N-terminus followed by a negatively charged aspartic acid residue, thus having two negative charges, one from the side chain and the other from the C-terminus. This peptide self-assembles in aqueous solution into 30–50 nm supramolecular structures [57]. Hexapeptides KTVIIE, STVIIE and KTVIIT have been shown to form fibrillar nanostructures only when the total net charge of the peptide is ±1 [58]. The net charge and the presence of several glutamic acids in Nab-Pc3c appear to favor aggregation and formation of fibrillar structures.

Conclusions

Aβ16–22, which has the ability to form fibrillar structures, is unable to induce β-structure when present at the N-terminus of amphipathic helical peptides, even in the presence of membrane-mimetic SDS micelles. Fibril formation appears to be inhibited when the peptides are dissolved in TFE, as observed from TEM. This could arise as the peptides may adopt helical conformation as in SDS micelles, despite the presence of Aβ16–22 in the sequence. When transferred to aqueous solutions, fibrillar structures are observed on prolonged incubation at RT, only when the peptide has a net charge of 0 and is not positively charged. The peptide that displays fibrillar structures exhibits β-structure by CD spectroscopy as well as enhancement in ThT fluorescence. Thus, it should be possible to generate organized nanostructures with hybrid peptides composed of amyloidogenic peptides and judiciously chosen amphipathic helices.

Acknowledgements

We acknowledge financial support from DST and CSIR, India under the project GAP301. S. R. thanks the Indian Academy of Sciences, Bangalore, for a summer fellowship. We thank Ms Madhumita Pattanayak and Dr Shashi Singh for help in TEM studies.

References

1 Park S-C, Kim J-Y, Shin S-O, Jeong C-Y, Kim M-H, Shin SY, 225Cheong G-W, Park Y, Hahm K-S. Investigation of toroidal pore and oligomerization by melittin using transmission electron microscopy. *Biochem. Biophys. Res. Comm.* 2006; **343**: 222–228.
2 Dhople VM, Nagaraj R. Conformation and activity of δ-lysin and its analogs. *Peptides* 2005; **26**: 217–225.
3 Verdon J, Girardin N, Lacombe C, Berjeaud J-M, Héchard Y. δ-hemolysin, an update on a membrane-interacting peptide. *Peptides* 2009; **30**: 817–823.
4 Saberwal G, Nagaraj R. Conformations of peptide fragments comprising the amino-terminal, central, and carboxyl-terminal regions of a membrane-active polypeptide: build-up of secondary structure in pardaxin. *J. Biol. Chem.* 1993; **268**: 14081–14089.
5 Porcelli F, Buck B, Lee D-K, Hallock KJ, Ramamoorthy A, Veglia G. Structure and orientation of pardaxin determined by NMR experiments in model membranes. *J. Biol. Chem.* 2004; **279**: 45815–45823.
6 Pan J, Nagle ST, Nagle JF. Alamethicin aggregation in lipid membranes. *J. Memb. Biol.* 2009; **231**: 11–27.
7 Oliynyk V, Jager M, Heimburg T, Buckin V, Kaatze U. Lipid membrane domain formation and alamethicin aggregation studied by calorimetry, sound velocity measurements, and atomic force microscopy. *Biophys. Chem.* 2008; **134**: 168–177.
8 Constantin D, Brotons G, Jarre A, Li C, Salditt T. Interaction of alamethicin pores in DMPC bilayers. *Biophys. J.* 2007; **92**: 3978–3987.
9 Kajava AV, Potekhin SA, Corradin G, Leapman RD. Organization of designed nanofibrils assembled from α-helical peptides as determined by electron microscopy. *J. Pept. Sci.* 2004; **10**: 291–297.
10 Xu Y, Shen J, Luo X, Zhu W, Chen K, Ma J, Jiang H. Conformational transition of amyloid β-peptide. *Proc. Natl. Acad. Sci. USA* 2005; **102**: 5403–5407.
11 Singh Y, Sharpe PC, Hoang HN, Lucke AJ, McDowall AW, Bottomley SP, Fairlie DP. Amyloid formation from an α-helix peptide bundle is seeded by 3,10-helix aggregates. *Chem. Eur. J.* 2011; **17**: 151–160 (and references therein).
12 Tjernberg LO, Callaway DJ, Tjernberg A, Hahne S, Lilliehook C, Terenius L, Thyberg J, Nordstedt C. A molecular model of Alzheimer amyloid beta-peptide fibril formation. *J. Biol. Chem.* 1999; **274**: 12619–12625.
13 Balbach JJ, Ishii Y, Antzutkin ON, Leapman RD, Rizzo NW, Dyda F, Reed J, Tycko R. Amyloid fibril formation by A beta 16–22, a seven-residue fragment of the Alzheimer's beta-amyloid peptide, and structural characterization by solid state NMR. *Biochemistry* 2000; **39**: 13748–13759.
14 Balbirnie M, Grothe R, Eisenberg DS. An amyloid-forming peptide from the yeast prion Sup35 reveals a dehydrated beta-sheet structure for amyloid. *Proc. Natl. Acad. Sci. USA* 2001; **98**: 2375–2380.
15 Cottingham MG, Hollinshead MS, Vaux DJT. Amyloid fibril formation by a synthetic peptide from a region of human acetylcholinesterase that is homologous to the Alzheimer's amyloid-β peptide. *Biochemistry* 2002; **41**: 13539–13547.
16 Reches M, Porat Y, Gazit E. Amyloid fibril formation by pentapeptide and tetrapeptide fragments of human calcitonin. *J. Biol. Chem.* 2002; **277**: 35475–35480.
17 Jones S, Manning J, Kad NM, Radford SE. Amyloid-forming peptides from beta2-microglobulin-insights into the mechanism of fibril formation in vitro. *J. Mol. Biol.* 2003; **325**: 249–257.
18 Nilsson MR, Dobson CM. In vitro characterization of lactoferrin aggregation and amyloid formation. *Biochemistry* 2003; **42**: 375–382.
19 Zanuy D, Ma B, Nussinov R. Short peptide amyloid organization: stabilities and conformations of the islet amyloid peptide NFGAIL. *Biophys. J.* 2003; **84**: 1884–1894.
20 Goux WJ, Kopplin L, Nguyen AD, Leak K, Rutkofsky M, Shanmuganandam VD, Sharma D, Inouye H, Kirschner DA. The formation of straight and twisted filaments from short tau peptides. *J. Biol. Chem.* 2004; **279**: 26868–26875.
21 Iwata K, Fujiwara T, Matsuki Y, Akutsu H, Takahashi S, Naiki H, Goto Y. 3D structure of amyloid protofilaments of 2-microglobulin fragment probed by solid-state NMR. *Proc. Natl. Acad. Sci. USA* 2006; **103**: 18119–18124.
22 Ivanova MI, Thompson MJ, Eisenberg D. A systematic screen of beta(2)-microglobulin and insulin for amyloid-like segments. *Proc. Natl. Acad. Sci. USA* 2006; **103**: 4079–4082.
23 Sawaya MR, Sambashivan S, Nelson R, Ivanova MI, Sievers SA, Apostol MI, Thompson MJ, Balbirnie M, Wiltzius JJ, McFarlane HT, Madsen AO, Riekel C, Eisenberg D. Atomic structures of amyloid cross-beta spines reveal varied steric zippers. *Nature* 2007; **447**: 453–457.
24 Hamley IW. Peptide fibrillization. *Angew. Chem. Int. Ed.* 2007; **46**: 8128–8147.
25 Favrin G, Irback A, Mohanty S. Oligomerization of amyloid Abeta16–22 peptides using hydrogen bonds and hydrophobicity forces. *Biophys. J.* 2004; **87**: 3657–3664.
26 Lu K, Jacob J, Thiyagarajan P, Conticello VP, Lynn DG. Exploiting amyloid fibril lamination for nanotube self-assembly. *J. Am. Chem. Soc.* 2003; **125**: 6391–6393.

27 Liang Y, Pingali SV, Jogalekar AS, Snyder JP, Thiyagarajan P, Lynn DG. Cross-strand pairing and amyloid assembly. *Biochemistry* 2008; **47**: 10018–10026.
28 Elgersma RC, Rijkers DT, Liskamp RM. pH controlled aggregation morphology of Abeta(16–22): formation of peptide nanotubes helical tapes and amyloid fibrils. *Adv. Exp. Med. Biol.* 2009; **611**: 239–240.
29 Tjernberg L, Hosia W, Bark N, Thyberg J, Johansson J. Charge attraction and β-propensity are necessary for amyloid fibril formation from tetrapeptides. *J. Biol. Chem.* 2002; **277**: 43243–43246.
30 Ma B, Nussinov R. Stabilities and conformations of Alzheimer's β-amyloid peptide oligomers (Aβ16–22, Aβ16–35, and Aβ10–35): sequence effects. *Proc. Natl. Acad. Sci. USA* 2002; **99**: 14126–14131.
31 Yamashita T, Takahashi Y, Takahashia T, Mihara H. Inhibition of peptide amyloid formation by cationic peptides with homologous sequences. *Bioorg. Medicinal Chem. Lett.* 2003; **13**: 4051–4054.
32 Chen Z, Krause G, Reif B. Structure and orientation of peptide inhibitors bound to beta-amyloid fibrils. *J. Mol. Biol.* 2005; **354**: 760–776.
33 Sharadadevi A, Sivakamasundari C, Nagaraj R. Amphipathic α-helices in proteins: results from analysis of protein structures. *Proteins: Structure, Function, and Bioinformatics* 2005; **59**: 791–801.
34 Sivakamasundari C, Nagaraj R. Interaction of 18-residue peptides derived from amphipathic helical segments of globular proteins with model membranes. *J. Biosci.* 2009; **34**: 239–250.
35 Atherton E, Sheppard RC. *Solid Phase Synthesis: A Practical Approach*. IRL Press: Oxford, 1989.
36 King DS, Fields CG, Fields GB. A cleavage method which minimizes side reactions following Fmoc solid phase peptide synthesis. *Int. J. Pept. Protein Res.* 1990; **36**: 255–266.
37 Naiki H, Higuchi K, Hosokawa M, Takeda T. Fluorometric determination of amyloid fibrils *in vitro* using the fluorescent dye, thioflavin T1. *Anal. Biochem.* 1989; **177**: 244–249.
38 Blanchard BJ, Thomas VL, Ingram VM. Mechanism of membrane depolarization caused by the Alzheimer Aβ1–42 peptide. *Biochem. Biophys. Res. Comm.* 2002; **293**: 1197–1203.
39 Blanchard BJ, Chen A, Rozeboom LM, Stafford KA, Weigele P, Ingram VM. Efficient reversal of Alzheimer's disease fibril formation and elimination of neurotoxicity by a small molecule. *Proc. Natl. Acad. Sci. USA* 2004; **101**: 14326–14332.
40 Konarkowska B, Aitken JF, Kistler J, Zhang S, Cooper GJS. The aggregation potential of human amylin determines its cytotoxicity towards islet β-cells. *FEBS J.* 2006; **273**: 3614–3624.
41 Sambasivam D, Liu CW, Jayaraman M, Malar EJP, Rajadas J. Aggregation and conformational studies on a pentapeptide derivative. *Biochim. Biophys. Acta* 2008; **1784**: 1659–1667.
42 Dusa A, Kaylor J, Edridge S, Bodner N, Hong D-P, Fink AL. Characterization of oligomers during α-synuclein aggregation using intrinsic tryptophan fluorescence. *Biochemistry* 2006; **45**: 2752–2760.
43 Bolognesi B, Kumita JR, Barros TP, Esbjorner EK, Luheshi M, Crowther DC, Wilson MR, Dobson CM, Favrin G, Yerbury JJ. ANS binding reveals common features of cytotoxic amyloid species. *ACS Chem. Biol.* 2010; **5**: 735–740.
44 Pawar AP, DuBay KF, Zurdo J, Chiti F, Vendruscolo M, Dobson CM. Prediction of "aggregation-prone" and "aggregation-susceptible" regions in proteins associated with neurodegenerative diseases. *J. Mol. Biol.* 2005; **350**: 379–392.
45 Kim W, Hecht MH. Generic hydrophobic residues are sufficient to promote aggregation of the Alzheimer's Aβ42 peptide. *Proc. Natl. Acad. Sci. USA* 2006; **103**: 15824–15829.
46 Pedersen JS, Dikov D, Otzen DE. N- and C-terminal hydrophobic patches are involved in fibrillation of glucagon. *Biochemistry* 2006; **45**: 14503–14512.
47 Zhang Z, Chen H, Lai L. Identification of amyloid fibril-forming segments based on structure and residue-based statistical potential. *Bioinformatics* 2007; **23**: 2218–2225 (and references therein).
48 Tian J, Wu N, Guo J, Fan Y. Prediction of amyloid fibril-forming segments based on a support vector machine. *BMC Bioinformatics* 2009; **10**(Suppl 1): S45.
49 Krysmann MJ, Castelletto V, Hamley IW. Fibrillisation of hydrophobically modified amyloid peptide fragments in an organic solvent. *Soft Matter* 2007; **3**: 1401–1406.
50 Krysmann MJ, Castelletto V, McKendrick JE, Clifton LA, Hamley IW, Harris PJF, King SM. Self-assembly of peptide nanotubes in an organic solvent. *Langmuir* 2008; **24**: 8158–8162.
51 Chaudhary N, Singh S, Nagaraj R. Organic solvent mediated self-association of an amyloid forming peptide from β2-microglobulin: an atomic force microscopy study. *Biopolymers (Pept Sci)* 2008; **90**: 783–791.
52 Castelletto V, Hamley IW, Harris PJF, Olsson U, Spencer N. Influence of the solvent on the self-assembly of a modified amyloid beta peptide fragment. I. Morphological investigation. *J. Phys. Chem. B* 2009; **113**: 9978–9987.
53 Hamley IW, Nutt DR, Brown GD, Miravet JF, Escuder B, Rodrı´guez-Llansola F. Influence of the solvent on the self-assembly of a modified amyloid beta peptide fragment. II. NMR and computer simulation investigation. *J. Phys. Chem. B* 2010; **114**: 940–951.
54 Shera JN, Sun XS. Effect of peptide sequence on surface properties and self-assembly of an amphiphilic pH-responsive peptide. *Biomacromolecules* 2009; **10**: 2446–2450.
55 Jun S, Hong Y, Imamura H, Ha B-Y, Bechhoefer J, Chen P. Self-assembly of the ionic peptide EAK16: the effect of charge distributions on self-assembly. *Biophys. J.* 2004; **87**: 1249–1259.
56 Castelletto V, Hamley IW, Cenker C, Olsson U. Influence of salt on the self-assembly of two model amyloid heptapeptides. *J. Phys. Chem. B* 2010; **114**: 8002–8008.
57 Vauthey S, Santoso S, Gong H, Watson N, Zhang S. Molecular self-assembly of surfactant-like peptides to form nanotubes and nanovesicles. *Proc. Natl. Acad. Sci. USA* 2002; **99**: 5355–5360.
58 López de la Paz M, Goldie K, Zurdo J, Lacroix E, Dobson CM, Hoenger A, Serrano L. De novo designed peptide-based amyloid fibrils. *Proc. Natl. Acad. Sci. USA* 2002; **99**: 16052–16057.

